Earth and Planetary Science Letters 460 (2017) 192–200

Contents lists available at ScienceDirect

Earth and Planetary Science Letters

www.elsevier.com/locate/epsl

Evidence for an impact-induced biosphere from the $\delta^{34}S$ signature of sulphides in the Rochechouart impact structure, France

S.L. Simpson [a,*], A.J. Boyce [b], P. Lambert [c], P. Lindgren [a], M.R. Lee [a]

[a] University of Glasgow, School of Geographical and Earth Sciences, Lilybank Gardens, G12 8QQ, Glasgow, UK
[b] Scottish Universities Environmental Research Centre, Rankine Ave, East Kilbride, G75 0QF, Glasgow, UK
[c] Sciences et Applications, 218 Boulevard Albert 1er, 33800 Bordeaux, France

ARTICLE INFO

Article history:
Received 11 March 2016
Received in revised form 13 December 2016
Accepted 16 December 2016
Editor: C. Sotin

Keywords:
rochechouart impact
impact hydrothermal
sulphur stable isotopes
bacterial sulphate reduction

ABSTRACT

The highly eroded 23 km diameter Rochechouart impact structure, France, has extensive evidence for post-impact hydrothermal alteration and sulphide mineralisation. The sulphides can be divided into four types on the basis of their mineralogy and host rock. They range from pyrites and chalcopyrite in the underlying coherent crystalline basement to pyrites hosted in the impactites. Sulphur isotopic results show that $\delta^{34}S$ values vary over a wide range, from −35.8‰ to +0.4‰. The highest values, $\delta^{34}S$ −3.7‰ to +0.4‰, are recorded in the coherent basement, and likely represent a primary terrestrial sulphur reservoir. Sulphides with the lowest values, $\delta^{34}S$ −35.8‰ to −5.2‰, are hosted within locally brecciated and displaced parautochthonous and autochthonous impactites. Intermediate $\delta^{34}S$ values of −10.7‰ to −1.2‰ are recorded in the semi-continuous monomict lithic breccia unit, differing between carbonate-hosted sulphides and intraclastic and clastic matrix-hosted sulphides. Such variable isotope values are consistent with a biological origin, via bacterial sulphate reduction, for sulphides in the parautochthonous and autochthonous units; these minerals formed in the shallow subsurface and are probably related to the post impact hydrothermal system. The source of the sulphate is likely to have been seawater, penecontemporaneous to the impact, as inferred from the marginal marine paleogeography of the structure. In other eroded impact craters that show evidence for impact-induced hydrothermal circulation, indirect evidence for life may be sought isotopically within late-stage (≤120 °C) secondary sulphides and within the shocked and brecciated basement immediately beneath the transient crater floor.

1. Introduction

1.1. Impact-generated hydrothermal systems

Meteorite impacts on rocky planetary bodies have the potential to initiate transient hydrothermal systems if: (i) the target contains sufficient volatiles (e.g. liquid water or ice), and (ii) a substantial heat source is generated (e.g. melt sheet, raised geothermal gradient) (Abramov and Kring, 2004; Naumov, 2005; Osinski et al., 2013; Koeberl, 2014). These impact-hydrothermal environments can host bacterial life, thus associated craters are promising targets in the search for evidence of water and exolife on other planets and satellites in our Solar System (Cockell and Bland, 2005; Naumov, 2005; Parnell et al., 2010b, 2012; Osinski et al., 2013; Sapers et al., 2014a). The lifetime of hydrothermal activity is contingent on the cooling rate of the structure (Naumov, 2005; Osinski et al., 2013); currently there are no active systems on Earth, and so our understanding of hydrothermal environments in craters is founded on what can be determined from the alteration products that are preserved within ancient systems.

Direct evidence for life may be sought in impact products, such as the microfossils found within the silicate glass of the Ries crater in Germany (Sapers et al., 2014a). However, the preservation of such evidence in many structures is often rare and compromised by diagenesis, weathering and erosion; parautochthonous impactites and the radial fracture network within the underlying and surrounding target rock can be all that remain of some ancient structures. Impact fractures are therefore likely to be optimum localities to search for evidence of life because convective heat transfer and hydrothermal fluid flow is focused within the fracture system as a result of the generally low permeability (<1 mD) of impact melt rocks and breccias (Parnell et al., 2010a).

Sulphides are a common hydrothermal product in impact craters and mineralisation is thought to occur during the latest

* Corresponding author.
E-mail address: ssimps56@uwo.ca (S.L. Simpson).

http://dx.doi.org/10.1016/j.epsl.2016.12.023

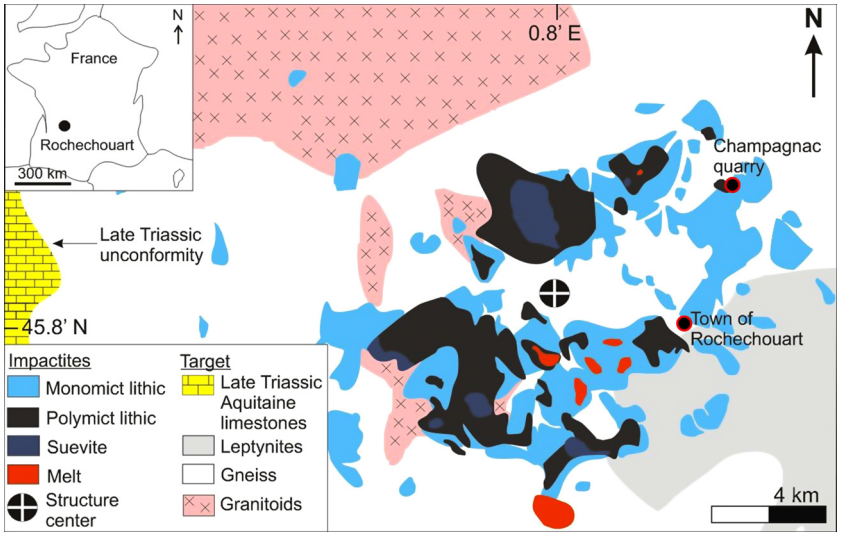

Fig. 1. Simplified geologic map of the Rochechouart impact structure, showing distribution of major impactites types and target lithologies. Modified after Lambert (2010) and the Bureau de Recherches Géologiques et Minières (BRGM), map numbers 686 and 687.

stages of cooling, when temperatures ($\leq$150 °C) become amenable to microbial metabolic processes (Machel, 2001; Cockell and Bland, 2005; Osinski et al., 2013). Previous studies of impact fractures have provided isotopic evidence for the formation of hydrothermal sulphide minerals as a by-product of bacterial sulphate reduction (Parnell et al., 2010b, 2012), for example, in the Haughton crater in Canada, which had a sulphate-rich, predominantly sedimentary target (Osinski et al., 2005).

In heavily eroded craters with evidence for impact-induced hydrothermal circulation, parautochthonous impactites and impact fractures beneath the transient crater floor may be a favourable location in which to seek geochemical evidence for the former presence of extremophiles. If thermophilic sulphate-reducing bacteria were present within the system, which contained a substantial source of sulphate and organic matter, it is likely that their presence will be captured isotopically within resultant sulphide minerals (Machel, 2001; Parnell et al., 2010b). The Rochechouart impact site offers such an opportunity, given its originally marginal marine setting and crystalline target, and significant sulphide mineralisation, which is well exposed in the Champagnac Quarry.

2. Materials and methods

2.1. The Rochechouart crater as an ideal laboratory

The 23 km diameter Rochechouart impact structure is located in west-central France, and has been dated to 203 $\pm$ 3 Ma (Lambert, 1977, 2010; *recalc.* Schmieder et al., 2010), thus placing it on the Triassic–Jurassic boundary. The target was marginal marine and located on the western edge of the Massif Central and north-eastern edge of the Aquitaine Basin (Lambert, 1977, 2010). Target rocks consist primarily of granitic metamorphic and intrusive igneous lithologies of the Variscan basement (Lambert, 1977, 2010). Rochechouart has been highly eroded; none of the original complex crater morphology is observed today, but enough material is preserved to provide a full suite of impactites that record various degrees of shock and mixing. All impactites have a pervasive hydrothermal overprint as K-metasomatism, argillic alteration and late stage carbonates (Lambert, 2010; Schmieder et al., 2010; Sapers et al., 2014b). A section through the transient crater floor-basement interface is accessible in Champagnac quarry (Fig. 1). This site thus offers an opportunity to study the effects of hydrothermal activity in the lower to sub-transient floor levels of a complex crater within a crystalline target.

The Champagnac site provides access to hydrothermally altered parautochthonous and autochthonous impactites, and minimally altered, coherent crystalline basement. In addition to the alteration assemblages noted by previous authors (Lambert, 2010; Sapers et al., 2014b), sulphide mineralisation is a feature of both the impactites and basement lithologies.

Here we have studied a crater in a marginal marine crystalline target in order to test the hypothesis that hydrothermal fluids within parautochthonous impactites and a basement impact fracture network can host extremophile microbial communities. Within the Champagnac site, we have sought to: (i) characterise the major types of aqueous alteration, with a focus on sulphides, within both impact and basement lithologies showing no macro- or microscopic evidence of shock metamorphism, using a range of imaging and spectroscopic techniques, and (ii) having described the paragenesis of the minerals, we then applied conventional and *in situ* laser S isotope analyses to examine the origins and interrelationships of the many sulphide deposits that occur below the transient crater floor.

2.2. Sample collection and characterisation

Fieldwork was undertaken in Champagnac quarry (Fig. 1) over the summers of 2013 and 2014. All of the sulphide-bearing impactite and basement lithologies were sampled, including a set of mineralised fractures of unknown origin within coherent and unshocked crystalline target rocks. Samples were examined in hand specimen, and polished thin sections were studied in transmitted and reflected light using an Olympus BX41 petrographic microscope. SEM imaging and energy dispersive X-ray (EDX) analyses were performed on rock chips and polished thin sections using two instruments, both housed within the University of Glasgow: a Carl Zeiss Sigma variable pressure analytical SEM, and a FEI Quanta 200F environmental SEM. They were operated at 20 kV and high vacuum. Prior to secondary electron (SE) imaging of approximately 1 cm^3 size chips, they were sputter coated with 10 nm of gold and further grounded using silver paint to reduce charging. To alleviate charging during SE and angle selective backscattered electron (AsB) imaging of the thin sections they were coated with 10 nm of carbon. EDX mapping and qualitative spot analysis was undertaken using an Oxford Instruments AZtec 2.2 SP1 system attached to the Zeiss SEM. The analyses were performed at a working distance of 8.5 to 11.5 mm and using a beam current of ~2 nA. X-ray maps

Table 1
Summary of Champagnac sulphides selected for isotopic analysis.

Host rock type	Sulphide type[a]	Mineral[b]	Description	Assc. minerals[b]
Semi-continuous monomict lithic breccia	1A	Pyr	3 to 5 mm, euhedral cubic pyrite associated with secondary calcite and dolomite matrix cement	Cal, Dol, Ort
	1B	Pyr	Sub-mm, irregular pyrite veins in clastic matrix	N/A
	1C	Pyr	Sub-mm, subhedral pyrite aligned within the fabric plane of monomict lithic breccia gneiss clasts	Dol, Qtz
Parautochthonous and autochthonous basement; locally brecciated and displaced	2	Pyr, Mar	Up to 5 mm-thick, massive, euhedral pyrite and marcasite coating impact fracture surfaces in sericitized granodiorite. Crystals display a variety of geometry and may be coated in a dusty-orange iron oxide crust	Cal, Dol, Qtz, Ox, Gyp, Phy, Ort
Coherent basement	3A	Pyr	2 to 3 mm, euhedral, cubic pyrite associated with partially melted K-feldspar in gneiss fabric	N/A
	3B	Pyr	Sub-mm, subhedral cubic pyrite aligned within gneiss fabric plane	N/A
	3C	Pyr	Up to 5 mm-thick, subhedral pyrite vein cross-cutting gneiss fabric	Dol
Basement fractures of unknown origin	4A	Cpy	1 to 2 mm, subhedral massive fracture coating chalcopyrite	Cal, Dol, Ort
	4B	Pyr, Cpy	4 to 5 mm, euhedral massive fracture coating pyrite and chalcopyrite	Cal, Dol, Ort

[a] See Section 3.1 for Type descriptions.
[b] Abbreviations: Cal = calcite; Cpy = chalcopyrite; Dol = dolomite; Gyp = gypsum; Mar = marcasite; Ort = orthoclase; Ox = iron oxides/hydroxides; Phy = phyllosilicates; Pyr = pyrite; Qtz = quartz.

were acquired at 1024 × 768 resolution with pixel dwell times ranging from 25 to 40 µs for acquisition periods of between 5 min and 5 h.

2.3. Stable isotope analysis

Samples were analysed for sulphur isotope ratios using both conventional gas extraction of hand-picked sulphides (Robinson and Kusakabe, 1975) and *in situ* laser combustion techniques (Wagner et al., 2002) at the Scottish Universities Environmental Research Centre (SUERC). Following combustion, purified SO_2 gases were analysed on a VG SIRA II mass spectrometer. Standard corrections were applied to raw $\delta^{66}SO_2$ to obtain true $\delta^{34}S$ values. Laser combustion produces a small degree of fractionation (typically <1‰) between extracted SO_2 gas and resulting mineral $\delta^{34}S$, which has been accounted for in all presented data (Wagner et al., 2002). Pyrite and marcasite, and pyrite and chalcopyrite species were extracted simultaneously and analysed together to obtain a bulk iron sulphide $\delta^{34}S$ value. All results are reported in permil (‰) notation relative to the Vienna Canyon Diablo Troilite standard (VCDT). Three sets of standards were repeatedly run during conventional sample analyses; international standards NBS-123 and IAEA-S-3, and an internal SUERC lab standard, CP1 (Wagner et al., 2002; Wacey et al., 2007). These standards yielded $\delta^{34}S$ values of +17.0‰, −31.6‰ and −4.1‰ (VCDT), respectively, versus accepted values of +17.1‰, −32.3‰ and −4.5‰. Reproducibility of standards during these analyses was typically equal to or better than ±0.3‰ (1σ).

3. Results

3.1. Mineralogy and sample classification

Pyrite, marcasite and chalcopyrite are the most common metal sulphides identified in this study. Four sulphide types can be recognised from their composition, host rock type, texture and ultimately, geologic context (Table 1). Detailed descriptions follow (Figs. 2–6), but they can broadly be described thus:

Type 1 sulphides are pyrites within the semi-continuous monomict lithic breccia, and are further subdivided based on geologic context into Type 1A, 1B and 1C;

Type 2 sulphides, pyrite and marcasite, are fracture-coating and vein forming massive sulphides and occur within the locally brecciated and fractured parautochthonous and autochthonous basement;

Type 3 sulphides, pyrite, are those found within coherent blocks of crystalline basement gneiss showing no macro- or microscopic shock features, and are further subdivided into Type 3A, 3B and 3C (Section 3.1.3);

Type 4 sulphides, pyrite and chalcopyrite, are those found within the mineralised basement fractures of unknown origin, and are subdivided into Type 4A and 4B (Section 3.1.4).

3.1.1. Monomict lithic breccia, Type 1 sulphides

The Champagnac-type monomict breccias are one of several discontinuous parautochthonous impactite bodies that occur throughout the Rochechouart structure (Fig. 1). They contain angular to sub-angular 1 to 4 cm size clasts that are composed of basement amphibolite gneiss, and have evidence for pervasive argillic alteration, moderate potassic alteration and late stage carbonate–sulphide mineralisation, which locally replaces the clastic matrix (Fig. 2) (Type 1A). Minor sulphide mineralisation occurs within the fabric plane of gneiss clasts (Type 1C) and within the clastic matrix, but lacks any preferred association with carbonates (Type 1B). Lithic clasts display ubiquitous adularia rims up to 250 µm thick (Fig. 5C–D) and in the vicinity of melt-bearing intrusions they may contain dark red-grey reaction rims of K-feldspar with soft clay interiors (Simpson et al., 2015a, 2015b).

3.1.2. Parautochthonous and autochthonous basement, Type 2 sulphides

Parautochthonous and autochthonous impactites are comprised of locally brecciated and displaced, poorly indurated, highly altered crystalline basement; they host considerable sulphide and carbonate mineralisation, more than any other impactite or target lithology at Champagnac. Veins are filled and fractures are coated with euhedral, 2 to 5 mm size pyrite crystals showing a variety of habits and microstructures. Bladed crystals of marcasite are scattered throughout the granodiorite host rock, and they are often associated with coarse, 1 to 3 mm size, euhedral Fe-rich dolomite rhombs (Fig. 3, Fig. 5A–B). The granodiorite host rock has been highly altered and contains a variety of phyllosilicates including muscovite, paragonite and minor chlorite; primary albite and K-feldspar display a pervasive sericitic texture. Outcrops display gossan, which is a red-orange iron oxide staining and highlights areas of particularly intense sulphide mineralisation (Fig. 3A).

3.1.3. Coherent basement, Type 3 sulphides

Basement amphibolite gneiss in Champagnac is minimally altered; this lithology has volumetrically minor iron sulphide mineralisation, pyrite (Table 1), that is aligned within the fabric plane

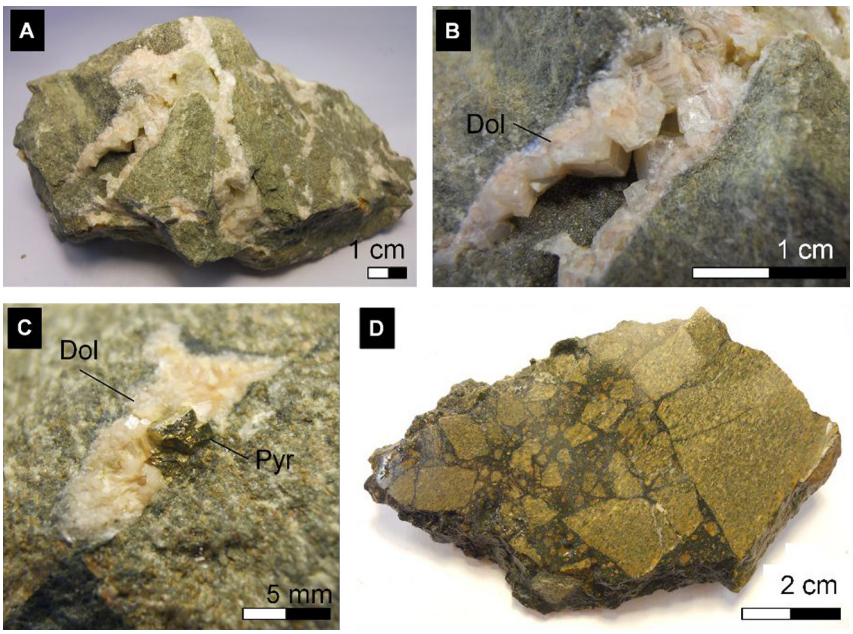

Fig. 2. Photographs of the monomict lithic impact breccia from Champagnac quarry. (A, B and C) Coarse–crystalline secondary carbonate–sulphide mineralisation (Type 1A), which locally completely replaces the clastic matrix. (D) Clean-cut surface of the Champagnac-type monomict lithic breccia, which has been altered by hydrothermal processes; the green–yellow colour of the lithic clasts is due to a secondary chlorite–smectite dominated mineral assemblage. Abbreviations: Dol = dolomite; Pyr = pyrite. (For interpretation of the references to colour in this figure legend, the reader is referred to the web version of this article.)

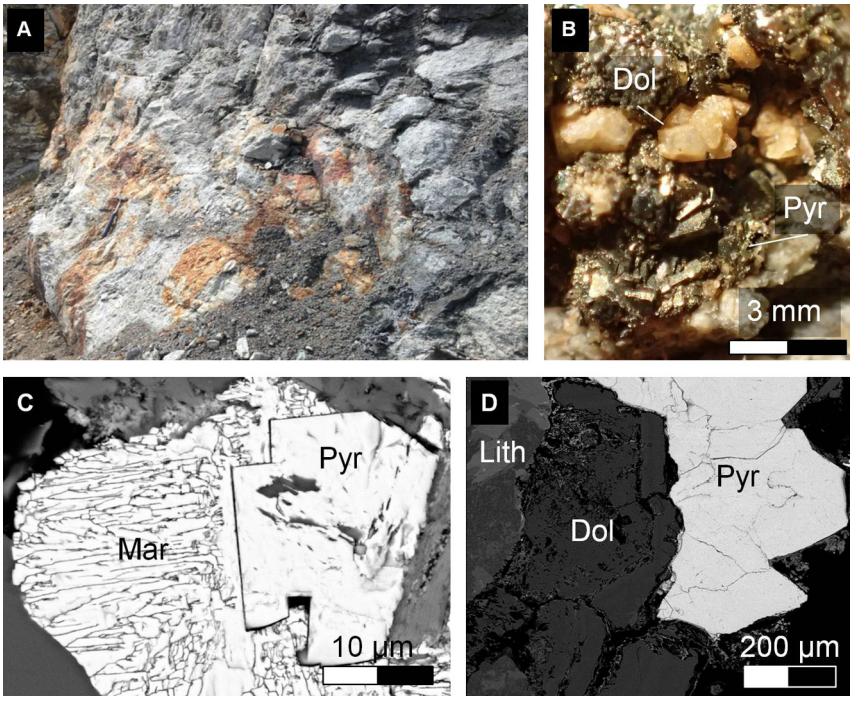

Fig. 3. (A) Photograph of iron oxide staining on an outcrop of sulphide-rich autochthonous impact fractures in Champagnac quarry, 7.5 km northeast of the structure's centre; (B) Photograph of typical fracture-coating sulphide–carbonate mineralisation in locally brecciated and fractured incoherent basement rocks, representative of Type 2 deposits (Table 1); (C and D) Backscattered SEM images of hydrothermal iron sulphides, pyrite and marcasite, and dolomite fracture coatings in locally brecciated parautochthonous basement from the Champagnac site (Type 2). Dolomite associated with heavy sulphide mineralisation is iron-rich and highly weathered. Abbreviations: Dol = dolomite; Lith = lithic clast; Mar = marcasite; Pyr = pyrite. (For interpretation of the references to colour in this figure, the reader is referred to the web version of this article.)

(Types 3A and 3B) and as small 2 to 3 mm size veins cross-cutting the gneiss fabric, sometimes associated with dolomite (Type 3C). Locally, the Upper and Lower Gneiss units contain formerly partially melted, bright red K-feldspar seen at the hand specimen scale, related to pre-impact exhumation during the Variscan orogeny. A sericitic texture also pervades primary feldspars; these phyllosilicates may represent pre-impact potassic alteration, as outlined by Lambert (2010) (Fig. 6).

3.1.4. *Basement fractures of unknown origin, Type 4 sulphides*

Sulphide mineralised fracture surfaces from within coherent blocks of minimally altered basement granodiorite were collected

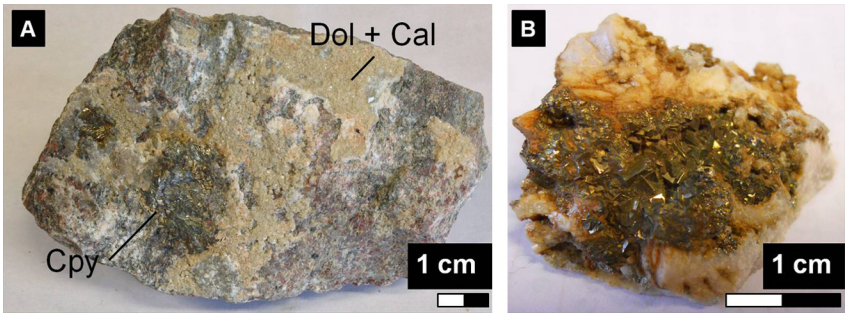

Fig. 4. (A) Photographs of mineralised basement fracture of unknown origin, or Type 4 sulphides, and (B) aggregate of euhedral pyrite and chalcopyrite crystals, also Type 4 (Table 2). Abbreviations: Cal = calcite; Cpy = chalcopyrite; Dol = dolomite.

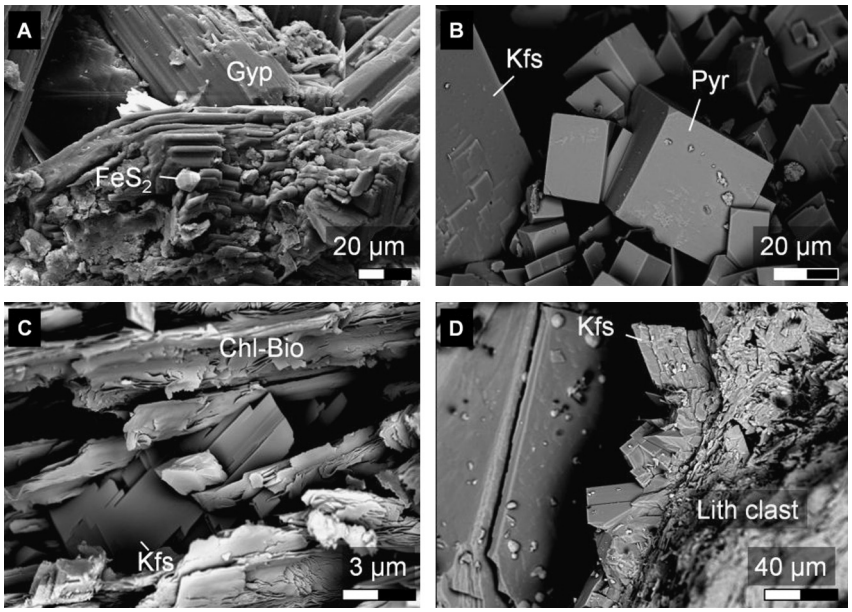

Fig. 5. Secondary electron SEM images of alteration within autochthonous and parautochthonous impactites in Champagnac. (A) Gypsum with minor iron sulphide crystal in autochthonous impact fracture coating (Type 2); (B) Euhedral, cubic pyrite and secondary K-feldspar within matrix of monomict lithic breccia (Type 1A); (C) Secondary K-feldspar growing between planes of mafic phyllosilicates in amphibolite gneiss clast of monomict breccia; and (D) euhedral adularia rim on lithic clast of monomict impact breccia. Abbreviations: Bio = biotite; Chl = chlorite; Gyp = gypsum; Kfs = K-feldspar; Pyr = pyrite.

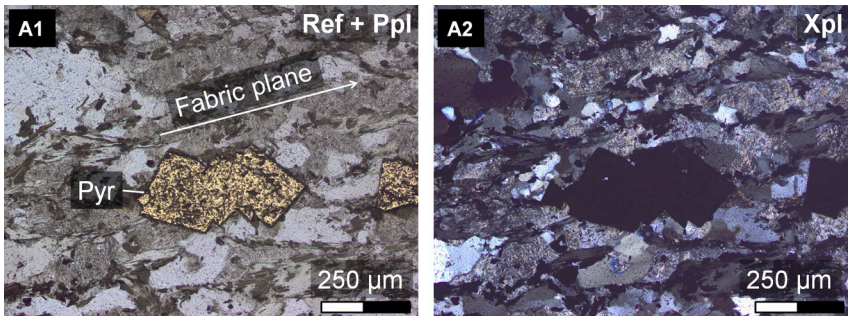

Fig. 6. Transmitted and reflected light images of pyrite within the fabric of unshocked amphibolite basement gneiss (Type 3B). $\delta^{34}S$ isotopic analysis reveals a significantly heavier sulphur reservoir, likely reflecting a primary terrestrial source; Type 3C sulphides that are associated with dolomite veins cross-cutting the gneiss fabric have slightly lower $\delta^{34}S$ values (~2 to 3‰) relative to Types 3A and 3B. Abbreviations: Ppl = plane polarised light; Pyr = pyrite; Ref = reflected light; Xpl = between crossed polarisers.

(Fig. 4). Type 4A sulphides are subhedral, 1 to 2 mm size crystals of chalcopyrite associated with calcite, dolomite and K-feldspar. Type 4B sulphides, pyrite and chalcopyrite, are slightly larger at 4 to 5 mm, and form crystal aggregates also associated with calcite, dolomite and K-feldspar. Because these fractures are hosted by coherent, crystalline basement the genetic relationship of the mineralisation therein to the impact event is unknown.

3.2. $\delta^{34}S$ isotope results

Twenty-three sulphide samples were selected for S isotopic analysis from Champagnac host rocks representing various degrees of macroscopic shock deformation and mixing of lithologies. Results show a wide range of $\delta^{34}S$ values ranging from as low as −35.8‰ in autochthonous impact fractures to +0.4‰ in the basement gneiss fabric (Table 2, Fig. 7).

Table 2
Summary of $\delta^{34}S$ results and standard data.

Sample	Rock and sample type[a]	Analysis type[b]	Mineral	$\delta^{34}S_{VCDT}$ (‰)
	Champagnac monomict lithic breccia			
MS-1	1A	Con	Pyr	−10.7
MS-2	1A	Con	Pyr	−5.6
MSL-1	1C	Laser	Pyr	−1.8
MSL-2	1B	Laser	Pyr	−1.2
	Parautochthonous and autochthonous basement			
AS-1	2	Con	Mar+Pyr	−32.0
AS-2	2	Con	Mar+Pyr	−31.8
AS-3	2	Con	Mar+Pyr	−32.2
AS-4	2	Con	Mar+Pyr	−34.2
AS-5	2	Con	Mar+Pyr	−35.5
AS-6	2	Con	Mar+Pyr	−35.8
AS-7	2	Con	Mar+Pyr	−26.9
ASL-1	2	Laser	Pyr	−5.20
ASL-2	2	Laser	Pyr	−24.6
ASL-3	2	Laser	Pyr	−18.5
	Coherent basement			
BS-1	3A	Con	Pyr	+0.4
BS-2	3C	Con	Pyr	−3.7
BSL-1	3B	Laser	Pyr	−1.0
BSL-2	3B	Laser	Pyr	−1.3
BSL-3	3C	Laser	Pyr	−2.7
	Basement fractures of unknown origin			
US-1	4A	Con	Cpy	−1.7
US-2	4A	Con	Cpy	−6.9
US-3	4B	Con	Cpy+Pyr	−26.2
US-4	4B	Con	Cpy+Pyr	−24.2

Standard	Mineral	Analysis type	Accepted values	This study
NBS-123	Sphalerite	Con	+17.1	+17
IAEAS-3	Argentite	Con	−32.3	−31.6
CP1	Chalcopyrite	Con	−4.5	−4.1

Reproducibility of standards equal to or better than ±0.3‰ (1σ).
[a] Refer to Table 1 for sample categorisation.
[b] Abbreviation: Con = conventional extraction and analysis (See methods); Cpy = chalcopyrite; Mar = marcasite; Pyr = pyrite.

4. Discussion

4.1. Fluid flow controls on sulphide mineralisation and $\delta^{34}S$ fractionation

The distribution, intensity and degree of hydrothermal alteration of Champagnac impactites indicate that this process was strongly influenced by their porosity and permeability. The highest intensity of carbonate–sulphide mineralisation is within autochthonous impact fractures (Type 2). Carbonate–sulphide mineralisation is less intense in the lithic breccias, where it only locally replaces the clastic matrix (Type 1A and 1B), and, even less commonly, is diffused throughout the fabric of gneiss clasts (Type 1C). A moderate degree of chloritisation and potassic alteration has affected all impactites. Apart from localised intrusions of hot, melt-bearing breccias, the mineral assemblages that are dominated by chlorite–smectite and carbonate–sulphide are typical of the intermediate to late stage and relatively cool (<150 °C) hydrothermal alteration in a complex crater, as outlined by Naumov (2005) and Osinski et al. (2013). The minor carbonate–sulphide mineralisation within the coherent, non-brecciated basement gneiss blocks is restricted to growth within the fabric plane, and as minor veins cross-cutting the fabric.

The hypothesis that post-impact convective flow of hydrothermal fluids is controlled by impact fracture networks (Parnell et al., 2010a) is corroborated by isotope results from Champagnac (Table 2, Fig. 7). The minima of sulphide $\delta^{34}S$ values (−35.8‰) is attained within autochthonous impact fractures and locally parautochthonous basement rocks (Type 2). This value is significantly lower than the range of all monomict breccia sulphides (Type 1;

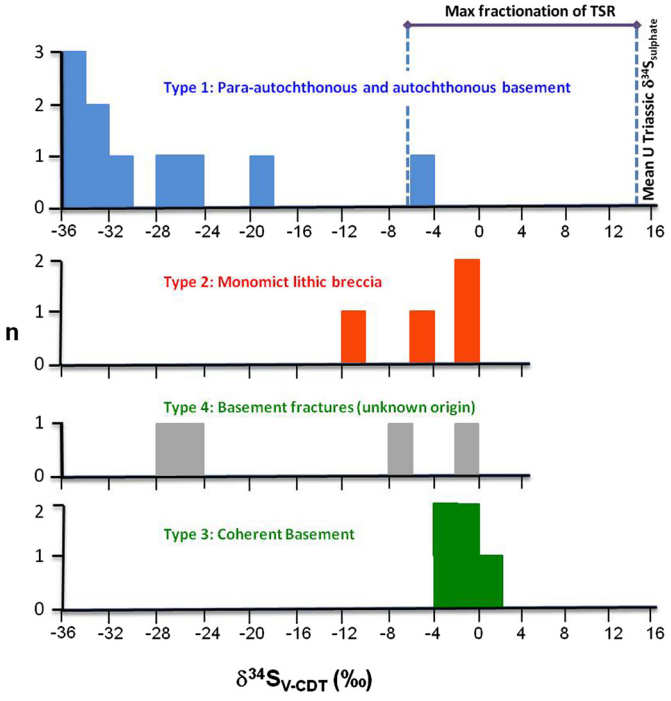

Fig. 7. Summary of $\delta^{34}S$ results. Mean Triassic seawater sulphate values from Longinelli and Flora (2007). Abbreviations: n = number of samples; TSR = thermochemical sulphate reduction.

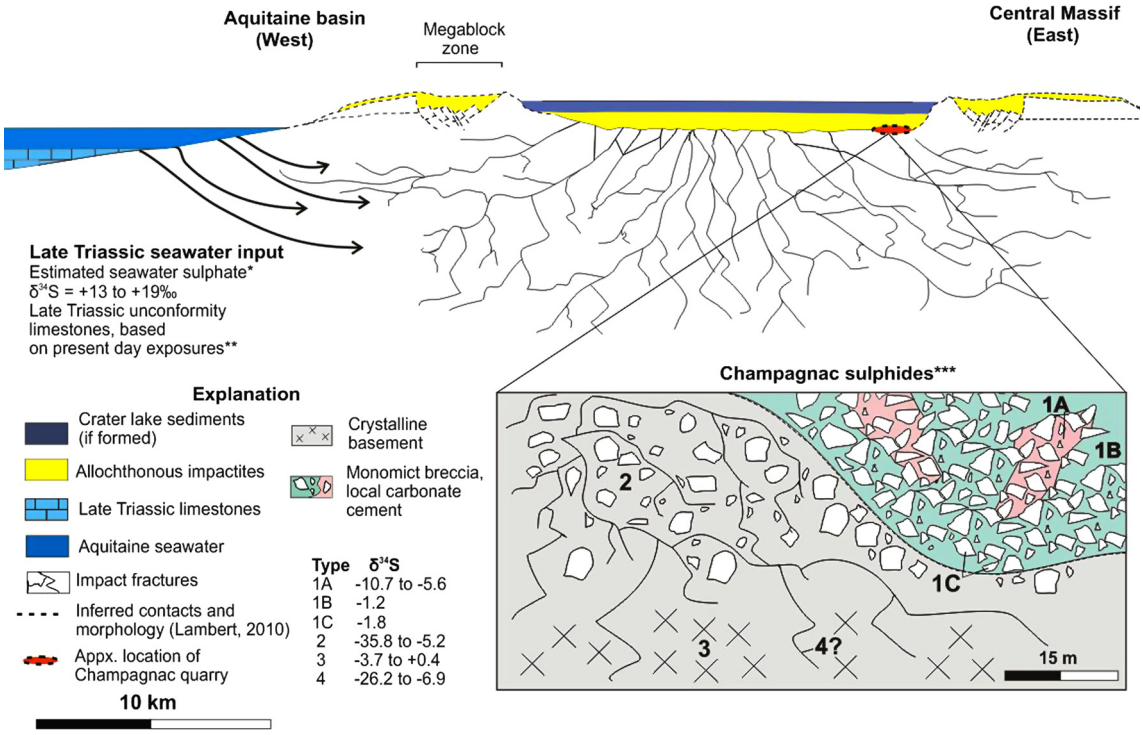

Fig. 8. Schematic cross-section through the Rochechouart structure during the Late-Triassic illustrating the influx of seawater along impact fractures. Also shown is a schematic cross-section through the Champagnac site with the geologic context of sulphide minerals and their respective δ^{34}S values. * = Values from Seal (2006). ** = Based on Lambert (2010) and the Bureau de Recherches Géologiques et Minières (BRGM), map numbers 686 and 687. *** = Full list of results found in Table 2.

δ^{34}S −10.7 to −1.2‰) and sulphides in coherent target rocks (Type 3; δ^{34}S −3.7 to +0.4‰). δ^{34}S values of pyrite within the metamorphic fabric of gneiss basement rocks falls within the range of igneous and sedimentary sulphur reservoirs (Type 3A and B) (Ohmoto and Rye, 1979; Seal, 2006; Labidi et al., 2012, 2013), although the isotopic homogeneity suggests a magmatic influence is more likely (Ohmoto and Rye, 1979; we note that the isotopic inhomogeneity in the entire system militates against any significant impactor S contribution, e.g. Tagle et al., 2009; Maier et al., 2006; Ripley et al., 2015). Similarly, only a minor degree of isotopic variation was recorded from the secondary basement veins (Type 3C). Given their setting in relation to the Variscan fabric, and the coincidence of the metamorphic pyrite S isotope values with the basement vein signatures, we speculate that vein sulphide may have been derived from remobilisation of original basement S. Sulphides from within the coherent basement gneiss rock fabric are likely to be Variscan in origin. However, without chronological constraints it is difficult to say for sure whether they are purely a product of Hercynian orogenesis.

Further evidence in support of the model for impact fracture-controlled fluid flow within and beneath the crater floor in Rochechouart comes from the comparison of sulphides within monomict lithic breccia clasts with their pre-impact equivalents in the coherent target gneiss. Post-impact hydrothermal activity has clearly affected the monomict lithic breccia, as evidenced by pervasive argillic and potassic alteration (Figs. 2, 5); however, these hydrothermal fluids appear to have left little imprint in the isotopic composition of sulphides within the non-porous clast fabric or clastic matrix. δ^{34}S values of sulphides are significantly lower only where the matrix is porous and has been replaced by a secondary carbonate cement (Table 2). Regardless of the origin of sulphides within the underlying target gneiss in Champagnac (i.e., Hercynian or post-Hercynian), impact hydrothermal activity has clearly not left its mark on the isotopic composition of sulphides within monomict breccia clast fabric to the same extent as it has affected those within the carbonate matrix cement or autochthonous impact fractures and parautochthonous brecciated basement.

Fracture-hosted sulphides within the basement granodiorite (Type 4) have a wide range of δ^{34}S values (−26.2‰ to −1.7‰; Table 2). It could be argued that samples US-3 and US-4 (−24.2‰ and −26.2‰, respectively) formed post-impact, as they certainly do not represent a primary, igneous or mantle-derived reservoir as seen in the target fabric sulphides (Seal, 2006; Labidi et al., 2012, 2013), and are similar to those in the autochthonous impact fractures and parautochthonous basement (Type 2). However, because they come from unshocked crystalline basement, their origin relative to the impact event is equivocal in the absence of chronological constraints.

4.2. Biological origin for sulphides precipitated within autochthonous impact fractures and parautochthonous basement rocks, and implications for hydrothermal fluid source

Conventional isotopic analyses reveal that the bulk sulphide minerals in autochthonous and parautochthonous impactites (Type 2) have δ^{34}S values that are considerably lower than in all other Champagnac lithologies (i.e., −35‰ to −26‰). Such negative values in a hydrothermal setting at diagenetic temperatures is reflective of authigenic sulphide precipitated from H_2S produced via sulphate reduction. To achieve such low values, this system must have been open with respect to the supply of sulphate. Considering the marginal marine paleogeography of Rochechouart, and the granitic crystalline target, seawater is the only fluid reservoir in this area during the late Triassic of sufficient size to have facilitated this process.

At present, basal Late-Triassic limestones occur less than 12 km west of the outermost preserved crater fill deposits (Lambert, 2010) (Fig. 1). Therefore we propose the infiltration of seawater into Rochechouart post-impact may have occurred in one of two ways; (i) via extensive impact fracturing of the crystalline basement, which would have reached the nearby sea (Fig. 8) or (ii) the

limestones preserved at the Aquitaine basin-Massif Central unconformity do not give an accurate representation of the shoreline during the Late Triassic, and the Mesozoic sea may have been closer than what can currently be deduced from local geology, possibly even covering the structure for a short period of time. However, crater fill impactite petrology, mineralogy and bulk geochemistry (Lambert, 2010; Sapers et al., 2014a) provide no evidence for substantial input from a sedimentary component, or inundation by seawater. Thus, scenario (ii) is unlikely. Further evidence in support of an impact fracture-assisted seawater infiltration model comes from the massive carbonate–sulphide hydrothermal assemblages and their corresponding biogenic sulphur isotopic signatures. These features are present in the parautochthonous and autochthonous impactites within and beneath the transient crater floor, as showcased at Champagnac, but are not observed in the allochthonous, relatively impermeable melt-bearing lithologies.

At relatively low temperatures ($\leq$150 °C) in an impact-hydrothermal environment, secondary sulphide minerals are likely to have precipitated directly from fluids. Metal cations, which were sourced from silicate hydrolysis and K-metasomatism during early to intermediate stages of impact-hydrothermal activity, would have reacted with H_2S produced from either thermochemical or bacterial sulphate reduction (TSR and BSR, respectively). Seawater sulphate $\delta^{34}S$ ranged from around +13‰ to +17.5‰ during the Upper Triassic, with a regional mean of around +15‰ (Longinelli and Flora, 2007). As abiotic TSR is only capable of reducing parent sulphate by a maximum of ~20‰, (Machel et al., 1995; Machel, 2001; Seal, 2006), the lowest limit for $\delta^{34}S$ in authigenic iron sulphide produced by TSR of marine sulphate in this area is ~−5‰ (we note that typical TSR fractionations are usually less than 20‰; Machel et al., 1995). Natural populations of sulphate-reducing bacteria may fractionate sulphur by as much as 72‰ (Seal, 2006; Wortmann et al., 2001; Sim et al., 2011; Stam et al., 2011; Leavitt et al., 2013). Moreover, the high spatial resolution laser data reveal significant fractionations at the mm-scale, as much as 20‰ within a single sample (ASL1 to 3, Table 2). Such heterogeneous isotopic distribution is characteristic of BSR, as opposed to TSR, which has a longer reaction rate resulting in generally homogeneous isotope fractionations (Machel, 2001). Lastly, TSR is common in high temperature diagenetic geologic environments and is a relatively slow process, requiring elevated temperatures of 100 to 180 °C over hundreds of thousands of years (Machel, 2001); hydrothermal models presented by Naumov (2005) and Osinski et al. (2013), as well as mineralogical evidence from Champagnac impactites, are incompatible with the homogeneous and sustained high temperatures required for TSR within this level of the structure. Based on these conclusions, the sulphur isotope data for sulphides within autochthonous impact fractures and parautochthonous basement rocks (Table 1) are consistent with a biological origin.

Previous authors have identified carbonate–sulphide mineralisation to be characteristic of late-stage hydrothermal activity in impact craters; isotope results from the present study corroborate this theory as the temperature limit for sulphate-reducing thermophilic microbes is between 0–80 °C, with only a small population of hyperthermophilic bacteria capable of surviving at temperatures up to 110 °C (Machel, 2001). We speculate that maximum activity of the sulphate reducing bacteria in this hydrothermal system would have occurred around 40–70 °C, since high H_2S production is observed in this range in hydrothermal vent sites, such as Guaymas Basin (Weber and Jorgensen, 2002). What remains unknown, as with the majority of impact-hydrothermal systems, is the longevity of fluid circulation and the extent to which it has affected the underlying, unshocked target rock. Future work on post-impact aqueous alteration in Rochechouart would thus benefit from the establishment of geochronological constraints, possibly by $^{40}Ar/^{39}Ar$ analysis of orthoclase that is ubiquitous throughout the structure.

5. Conclusion

The distribution of hydrothermal sulphides and their corresponding levels of sulphur isotope fractionation in impactites from the Champagnac quarry directly correlate with host rock porosity and permeability. Hydrothermal authigenic iron sulphides within autochthonous impact fractures and locally brecciated basement (Type 2) show the greatest isotopic fractionations, with bulk values as low as −35.8‰ (VCDT). Post-impact hydrothermal activity has affected the semi-continuous monomict parautochthonous impact breccias, as evidenced by changes in bulk mineralogy. Alteration has had a negligible effect on the isotopic composition of sulphides within the clast fabric or clastic matrix (Type 1B and 1C), whose $\delta^{34}S$ values parallel those within the coherent target, reflecting a heavier, primary sulphur reservoir and are likely to have been inherited directly from the crystalline basement gneiss; only authigenic secondary pyrite associated with the matrix carbonate cement (Type 1A) has significantly fractionated $\delta^{34}S$.

There is strong evidence that the impact-induced fracture network within Rochechouart supported sulphur-reducing bacteria during post-impact hydrothermal activity, as indicated by the highly negative $\delta^{34}S$ values of authigenic sulphides therein, the heavier, primary sulphur reservoir of crystalline target rocks, and the large, heterogeneous fractionations at the small scale revealed by microanalysis. Such a high degree of negative fractionation is characteristic of BSR, as opposed to TSR, and requires an open supply of sulphate; along with the ubiquitous presence of dolomite and marginal marine paleogeography, isotope results support a mixing model for hydrothermal fluids including seawater in Rochechouart.

Results from this study suggest that in those hydrothermally altered impact structures where access to crater-fill lithologies may be limited, for example due to erosion, the fracture network within and beneath the crater floor may preserve evidence for microbial colonisation during the cooling period.

Acknowledgements

This research was funded by the Barringer Family Fund for Meteorite Impact Research, awarded to Sarah Simpson. We also acknowledge funding from the UK Science and Technology Facilities Council through grant ST/K000942/1. AJB is funded by Natural Environment Research Council support of the Isotope Community Support Facility at SUERC through contract R8/H10/76. The authors would also like to thank the laboratory staff at SUERC and the technicians based at the University of Glasgow for their assistance with isotopic analysis, SEM measurements and sample preparation, as well as the staff at the Réserve Naturelle Nationale de l'Astroblème de Rochechouart–Chassenon for welcoming us to their park, their assistance in the field, and for granting us permission to sample from the structure.

References

Abramov, O., Kring, D., 2004. Numerical modelling of an impact-induced hydrothermal system at the Sudbury crater. J. Geophys. Res. 109, E10007.

Bureau de recherché géologiques et minières, 1982. Maps: number 686: La Rochefoucauld, number 687: Rochechouart, 2012. 1:50,000. BRGM.

Cockell, C.S., Bland, P.A., 2005. The evolutionary and ecological benefits of asteroid and comet impacts. Trends Ecol. Evol. 20 (4), 175–179.

Koeberl, C., 2014. The geochemistry and cosmochemistry of impacts. In: Planets, Asteroids, Comets and The Solar System. In: Treatise on Geochemistry, vol. 2, 2nd edition. Elsevier, pp. 73–118.

Labidi, J., Cartigny, P., Birck, J.L., Assayag, N., Bourrand, J.J., 2012. Determination of multiple sulfur isotopes in glasses: a reappraisal of the MORB $\delta^{34}S$. Chem. Geol. 334, 189–198.

Labidi, J., Cartigny, P., Moreira, M., 2013. Non-chondritic sulphur isotope composition of the terrestrial mantle. Nature 501, 208–211.
Lambert, P., 1977. The Rochechouart Crater: shock zoning study. Earth Planet. Sci. Lett. 35, 258–268.
Lambert, P., 2010. Target and impact deposits at Rochechouart impact structure, France. Spec. Pap., Geol. Soc. Am. 465.
Leavitt, W.D., Halevy, I., Bradley, A.S., Johnston, D.T., 2013. Influence of sulfate reduction rates on the Phanerozoic sulfur isotope record. Proc. Natl. Acad. Sci. USA 110, 11244–11249.
Longinelli, A., Flora, O., 2007. Isotopic composition of gypsum samples of Permian and Triassic age from the north-eastern Italian Alps: palaeoenvironmental implications. Chem. Geol. 245, 275–284.
Machel, H.G., 2001. Bacterial and thermochemical sulfate reduction in diagenetic settings – old and new insights. Sediment. Geol. 140, 143–175.
Machel, H.G., Krouse, H.R., Sassen, R., 1995. Products and distinguishing criteria of bacterial and thermochemical sulfate reduction. Appl. Geochem. 10, 373–389.
Maier, W.D., Andreoli, M., McDonald, I., Higgins, M.D., Boyce, A.J., Shukolyukov, A., Lugmair, G.W., Ashwal, L.D., Graeser, P., Ripley, E., Hart, R., 2006. Discovery of a 25 cm asteroid clast in the giant Morokweng impact crater, South Africa. Nature 441, 203–206.
Naumov, M., 2005. Principal features of impact-generated hydrothermal circulation systems: mineralogical and geochemical evidence. Geofluids 5, 165–184.
Ohmoto, H., Rye, R.O., 1979. Isotopes of sulfur and carbon. In: Barnes, H.I. (Ed.), Geochemistry of Hydrothermal ore Deposits, 2nd edition. Wiley, New York, pp. 509–567.
Osinski, G.R., Lee, P., Parnell, J., Spray, J.G., Baron, M., 2005. A case study of impact-induced hydrothermal activity: the Haughton impact structure, Devon Island, Canadian High Arctic. Meteorit. Planet. Sci. 40, 1859–1877.
Osinski, G.R., Tornabene, L.T., Banerjee, N.R., Cockell, C.S., Flemming, R., Izawa, M.R., McCutcheon, J., Parnell, J., Preston, L.J., Pickersgill, A.E., Pontefract, A., Sapers, H., Southam, G., 2013. Impact-generated hydrothermal systems on Earth and Mars. Icarus, 347–363.
Parnell, J., Taylor, W.C., Thackrey, S., Osinski, G.R., Lee, P., 2010a. Permeability data for impact breccias imply focussed hydrothermal fluid flow. J. Geochem. Explor. 106, 171–175.
Parnell, J., Boyce, A., Thackrey, S., Muirhead, D., Lindgren, P., Mason, C., Taylor, C., Still, J., Bowden, S., Osinski, G.R., Lee, P., 2010b. Sulfur isotope signatures for rapid colonization of an impact crater by thermophilic microbes. Geology 38, 271–274.
Parnell, J., Boyce, A.J., Osinski, G.R., Izawa, M.R.M., Banerjee, N., Flemming, R., Lee, P., 2012. Evidence for life in the isotopic analysis of surface sulphates in the Haughton impact structure, and potential application on Mars. Int. J. Astrobiol. 11, 91–101.
Ripley, E.M., Lightfoot, P.C., Stifter, E.C., Underwood, B., Taranovic, V., Dunlop III, M., Donnghue, K.A., 2015. Heterogeneity of S isotope compositions recorded in the Sudbury Igneous Complex, Canada: significance to formation of Ni–Cu sulfide ores and the host rocks. Econ. Geol. 110, 1125–1135.
Robinson, B.W., Kusakabe, M., 1975. Quantitative preparation of sulphur dioxide for $^{34}S/^{32}S$ analyses from sulphides by combustion with cuprous oxide. Anal. Chem. 47, 1179–1181.
Sapers, H.M., Osinski, G.R., Banerjee, N.R., Preston, L.J., 2014a. Enigmatic tubular features in impact glass. Geology 42 (6), 471–474.
Sapers, H.M., Osinski, G.R., Banerjee, N.R., Ferriere, L., Lambert, P., Izawa, M.R., 2014b. Revisiting the Rochechouart impact structure, France. Meteorit. Planet. Sci., 1–17.
Schmieder, M., Buchner, E., Schwarz, W.H., Trieloff, M., Lambert, P., 2010. A Rhaetian $^{40}Ar/^{39}Ar$ age for the Rochechouart impact structure (France) and implications for the latest Triassic sedimentary record. Meteorit. Planet. Sci. 45, 1225–1242.
Seal, R., 2006. Sulfur isotope geochemistry of sulfide minerals. Rev. Mineral. Geochem. 61 (1), 633–677.
Sim, M.S., Bosak, T., Ono, S., 2011. Large sulfur isotope fractionation does not require disproportionation. Science 333, 74–77.
Simpson, S.L., Lambert, P., Lee, M.R., 2015a. Evidence for localized high temperature hydrothermal fluid flow within the sub-crater environment of the Rochechouart impact structure: observations from a polymict breccia dike. Lunar Planet Sci. Conf. 46, 1751.
Simpson, S.L., Boyce, A.J., Lambert, P., Lee, M.R., Lindgren, P., 2015b. Stable isotope studies of the Rochechouart impact structure: sources of secondary carbonates and sulphides within allochthonous and parautochthonous impactites. Lunar Planet Sci. Conf. 46, 1740.
Stam, M.C., Mason, P.R.D., Laverman, A.M., Pallud, C., Van Cappellen, P., 2011. $^{34}S/^{32}S$ fractionation by sulfate-reducing microbial communities in estuarine sediments. Geochim. Cosmochim. Acta 75, 3903–3914.
Tagle, R., Schmitt, R.T., Erzinger, J., 2009. Identification of the projectile component in the impact structures Rochechouart, France and Sääksjärvi, Finland: implications for the impactor population for the Earth. Geochim. Cosmochim. Acta 73, 4891–4906.
Wacey, D., Wright, D., Boyce, A., 2007. A stable isotope study of microbial dolomite formation in the Coorong Region, South Australia. Chem. Geol. 244, 155–174.
Wagner, T., Boyce, A.J., Fallick, A.E., 2002. Laser combustion analysis of ^{34}S of sulfosalt minerals: determination of the fractionation systematics and some crystal-chemical considerations. Geochim. Cosmochim. Acta 66, 2855–2863.
Weber, A., Jorgensen, B.B., 2002. Bacterial sulfate reduction in hydrothermal sediments of the Guaymas Basin, Gulf of California, Mexico. Deep-Sea Res., Part 1 49, 827–841.
Wortmann, U.G., Bernasconi, S.M., Bötcher, M.E., 2001. Hypersulfidic deep biosphere indicates extreme sulphur isotope fractionation during single-step microbial sulphate reduction. Geology 29, 647–650.